COMMUNICATION www.rsc.org/chemcomm | ChemComm

Transformable periodic mesoporous organosilica materials†

Steven E. Dickson and Cathleen M. Crudden*

Received (in Berkeley, CA, USA) 23rd November 2009, Accepted 25th January 2010
First published as an Advance Article on the web 16th February 2010
DOI: 10.1039/b924570g

The synthesis of novel periodic mesoporous organosilica (PMO) materials incorporating a mixture of functional monomers (*cis*- and *trans*-stilbene-based) and structural monomers has been accomplished. EDX analysis of these materials in combination with HAADF imaging of OsO_4-stained samples reveals a homogeneous distribution of *trans*-olefin within the co-condensed aromatic organosilica matrix. Ozonolysis of the functional component demonstrates the significant potential of this material for further modification.

Periodic mesoporous organosilicas (PMOs)[1] have received considerable attention since they were first reported in 1999, due in large part to the potential for introducing a wide variety of structures into the backbone of the material *via* organic spacers of the monomer unit $[(R'O)_3Si–R–Si–(OR')_3]$.[2] Unlike conventional modifications of mesoporous silica phases that rely on grafting of siloxanes onto the surface, PMOs can be prepared with high loadings of the functional group, distributed homogeneously throughout the bulk of the material. In addition to imparting interesting properties such as increased hydrophobicity or enhanced hydrothermal stability, incorporating the organic fragment into the wall of the silica matrix circumvents the commonly associated problem of pore diameter reduction or blockage following post synthetic modifications, which may limit the interactions of guest molecules. Finally, as we will demonstrate, significant modifications can be made to the organic core in the case of the PMO materials that result in uniformly distributed organic functionality.

Despite the number of reports addressing the design of PMOs, the majority of these are based on aromatic or precursors having short, rigid structures. Unfortunately, these linkers offer limited reactivity and therefore, with few exceptions,[3] have seen limited use in further modifications.

In this communication, we report a novel approach to the synthesis of PMOs based on the use of two types of monomers, one which is meant to impart function or to provide a handle for the introduction of further functionality, and one which is present for structural stability. We recently described a related material in which the functional component was a chiral biaryl unit and the structural, an achiral biaryl monomer.[4] Herein, we describe a system in which a stilbene-based monomer (*trans* or *cis*) (**1** and **2**) can be co-incorporated with benzene- or biphenyl-bridged monomers (**3** and **4**) as the structural elements (Scheme 1). The stilbene unit was chosen because of the large number of transformations that this substructure is known to undergo, as well as the possibility of accessing different conformations or morphologies from the *cis* and *trans* isomers.

To prepare the *trans*-stilbene functional monomer (**1**), a Grubbs olefination reaction was employed which results in the dimerization of 4-bromostyrene with loss of ethylene in quantitative yield.[5] Conversion of the bromo substituents to iodides[6] is then followed by a Masuda coupling[7] to introduce the polymerizable siloxane units (Scheme 2). For the more synthetically challenging *cis* isomer (**2**), a lithium-free Wittig reagent was prepared by reaction between triphenylphosphine and 4-bromobenzylbromide followed by deprotonation with KOH.[8] Treatment with 4-bromobenzaldehyde affords *cis*-4,4′-dibromostilbene in 72% yield with 80% stereochemical control. Following halogen exchange, the siloxane units were installed using the Masuda reaction as described above (see ESI†).

PMO materials were then prepared by mixing the functional monomer (**1** or **2**) along with either 1,4-bis(triethoxysilyl)-benzene (**3**) or 4,4′-bis(triethoxysilyl)biphenyl (**4**) as the structural component, in the presence of a structure directing template (small or large pore-producing) under acidic or basic conditions (see ESI†). The synthetic conditions and resulting nitrogen adsorption data are shown in Tables 1 and 2 respectively.

The PMOs prepared exhibited Type IV isotherms with moderate to high surface areas and narrow pore size distributions. **PMO-1/4$^{H^+}$** and **PMO-2/4$^{H^+}$** made with Brij® 76 surfactant displayed type H4 hysteresis loops that do not close at low

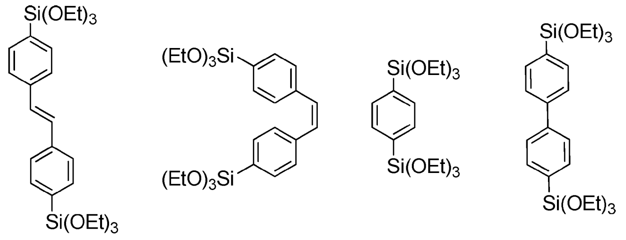

1 **2** **3** **4**

Scheme 1 (**1**) 4,4′-Bis(triethoxysilyl)*trans*-stilbene **BTETS**; (**2**) 4,4′-bis(triethoxysilyl)*cis*-stilbene **BTECS**; (**3**) 1,4-bis(triethoxysilyl)-benzene **BTEB**; (**4**) 4,4′-bis(triethoxysilyl)biphenyl **BTEBP**.

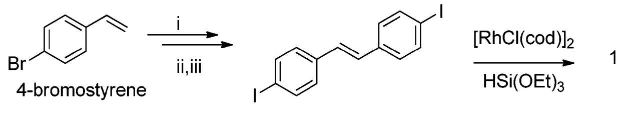

Scheme 2 (i) Grubbs catalyst (2nd Gen.), CH_2Cl_2, room temp. 16 h; (ii) *n*-BuLi, THF, −78 °C, 30 min and (iii) I_2, −78 °C to room temp. 16 h.

---

*Department of Chemistry, Queen's University, 90 Bader Lane, Kingston, Ontario, Canada K7L 3N6.
E-mail: cruddenc@chem.queensu.ca; Fax: +1-613533-6669;
Tel: +1-613533-6000*

† Electronic supplementary information (ESI) available: Material preparations and characterizations including N_2 isotherms, CP MAS NMR spectra and XRD patterns are available. See DOI: 10.1039/b924570g

Table 1 Synthesis of PMO materials using stilbene and benzene or biphenyl-based monomers[a]

Material	Functional monomer	Structural monomer	Template	pH
PMO-1/4$^{H^+}$	**1**	**4**	Brij® 76	Acidic
PMO-1/4$^{OH^-}$	**1**	**4**	C_{18}TMACl	Basic
PMO-2/4$^{H^+}$	**2**	**4**	Brij® 76	Acidic
PMO-1/3$^{H^+}$	**1**	**3**	P123	Acidic

[a] Molar ratios: **PMO-1/4**$^{H^+}$ (**1** : **4** : Brij® 76 : H_2O : HCl : NaCl) (0.15 : 0.85 : 0.534 : 601 : 8.05 : 19.0);[9] **PMO-1/4**$^{OH^-}$ (**1** : **4** : C_{18}TAMCl : H_2O : NaOH) (0.15 : 0.85 : 1.28 : 1320 : 12 100);[10] **PMO-2/4**$^{H^+}$ (**2** : **4** : Brij® 76 : H_2O : HCl : NaCl) (0.15 : 0.85 : 0.534 : 601 : 8.05 : 19.0);[9] **PMO-1/3**$^{H^+}$ (**1** : **3** : P123 : HCl : H_2O) (0.15 : 0.85 : 0.068 : 0.944 : 800).[11]

Table 2 Textural properties of prepared PMOs

Material	BET surface area/m^2 g^{-1}	Pore diameter[a]/Å	Pore volume[a]/cm^3 g^{-1}
PMO-1/4$^{H^+}$	1009	27	0.75
PMO-1/4$^{OH^-}$	694	20	0.40
PMO-2/4$^{H^+}$	952	26	0.65
PMO-1/3$^{H^+}$	282	74	0.85

[a] Calculated from BJH adsorption branch.

P/P_0, which could be indicative of slit-like pores.[12] **PMO-1/3**$^{H^+}$ synthesized using P123 as surfactant exhibited a nitrogen adsorption profile typical of SBA-15 (see ESI†).

TEM images show that although **PMO-1/4**$^{H^+}$ and **PMO-1/4**$^{OH^-}$ appear to have less ordered worm-hole type pore structures, the other two materials have well-organized, mesoporous structures (Fig. 1). CP MAS ^{29}Si NMR spectra are characterized by T^1, T^2 and T^3 sites, with no evidence of Q sites, indicating Si–C bond retention under all synthetic conditions studied. Materials were also prepared with 30% and 100% of the functional monomer **1** using P123 as the surfactant under acidic conditions. It was found that at these higher concentrations, the stilbene precursor hydrolyzes readily to the bis(silanetriol), which forms large crystals instead of condensing as indicated by CP MAS ^{29}Si NMR and TEM analysis (see ESI†). While at 30% loading, the material was characterized by a mixture of crystalline and condensed material, at 100% loading of the stilbene monomer, only crystals were present, as observed by TEM or inspection under a regular optical microscope (see ESI†). This has been observed previously by Corriu and co-workers by hydrolysis of **1** in a biphasic medium of ether and aqueous HCl.[13] Interestingly, despite the fact that our conditions were harsher than those of Corriu *et al.*, no triol was observed when **PMO-1/4**$^{H^+}$ was prepared using 15% loading of **1** relative to **4**. This suggests that at least 15% (but not 30%) of **1** can be incorporated into a PMO with **3** without forming detectable amounts of bis(silanetriol).

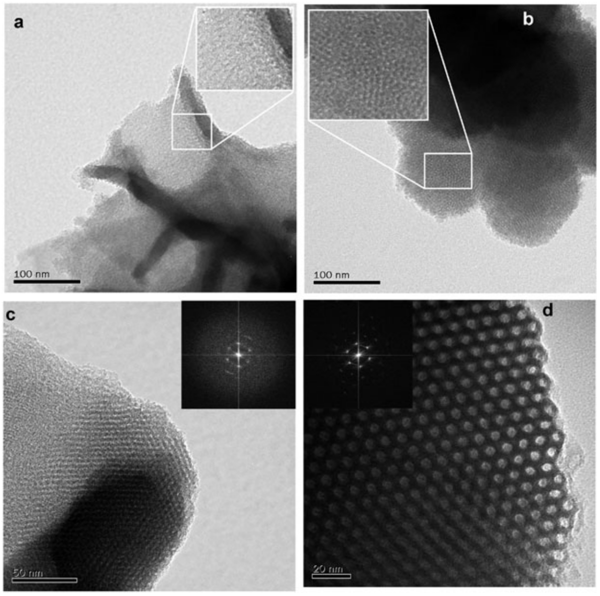

Fig. 1 TEM images of (a) **PMO-1/4**$^{H^+}$, (b) **PMO-1/4**$^{OH^-}$, (c) **PMO-2/4**$^{H^+}$ and (d) **PMO-1/3**$^{H^+}$. Insets of (a) and (b) show close-up of pore structure and (c) and (d) are electron diffraction patterns.

An important question to be addressed with mixed PMO systems is the degree of homogeneity of the various components within the final material.[14] To probe this question, **PMO-1/3**$^{H^+}$ containing 15% functional monomer **1** was treated with OsO_4 vapour in a closed jar, and allowed to react for 4 h at room temperature (Scheme 3). As OsO_4 reacts selectively with olefins and (under these conditions) remains bound to the olefin in the form of an osmate ester, we employed this as a marker for the stilbene component of the PMO. TEM imaging under high angle annular dark field conditions (HAADF) is highly sensitive to atomic number (known as Z-contrast imaging) and in combination with energy dispersive X-ray spectroscopy (EDX), the presence and general distribution of Os within the organosilica matrix was determined. Treatment of **PMO-1/3**$^{H^+}$ with OsO_4 resulted in a material with highly dispersed Os, as determined by HAADF imaging. Because the Os was so well dispersed, we carried out a control experiment by mixing two batches of material, one that was stained and one that was not, on the same TEM grid. The unstained material was prepared by condensing purely structural monomer **3**, which contained no olefin, and reacting it with OsO_4. This provided an additional control which was the determination of whether OsO_4 would merely adsorb to the unfunctionalized material.

As can be seen in Fig. 2, particles with uniformly high contrast were observed in addition to particles with much lower contrast (Fig. 2a and b). The presence of osmium in the high-contrast particles and the absence in the lower-contrast particles was further confirmed by examination of the EDX spectra of the two types of particles (Fig. 2c and d). It should be noted that for each of the individual samples, the same EDX spectrum was observed at various beam locations.

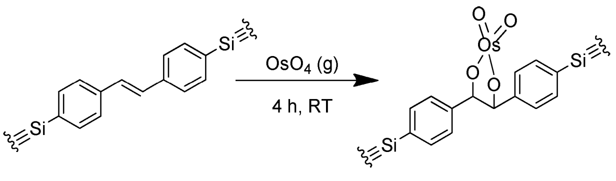

Scheme 3

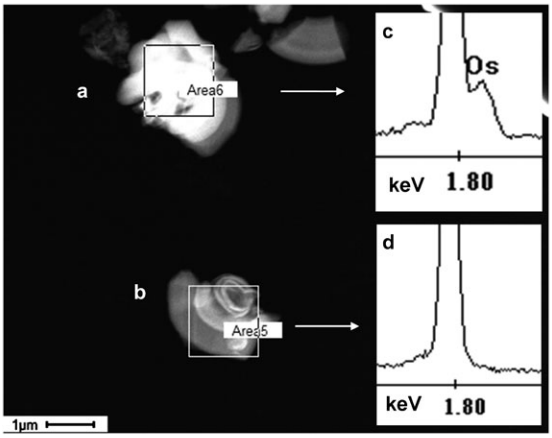

Fig. 2 HAADF images of a mixed sample of (a) **PMO-1/3$^{H^+}$-Os** and (b) control particles. Brightest areas indicate the presence of Os atoms. The insets (c) and (d) are EDX spectra showing the presence of Os in (a), but not in (b).

Distinct Os M lines can be found at 1.96 keV overlapping slightly with Si K lines. Deconvolution of the peaks confirmed that the ratio of peak intensity of Os M to Si K was consistent in all locations tested. This supports a homogeneous distribution of the stilbene component within the organosilica material.

As a test for determining the accessibility of the functional monomers within the material, **PMO-1/3$^{H^+}$** was subjected to ozonolysis conditions at −78 °C, followed by a reductive workup with Me_2S. This procedure is known to cleave similar olefins, resulting in two aryl aldehydes.[15] Infrared spectroscopy supported the effectiveness of this reaction as a new band appeared at 1700 cm^{-1}, which is diagnostic of an aromatic aldehyde. Furthermore, this treatment appeared to *completely* oxidize the olefin of **4** as determined *via* confocal micro-Raman spectroscopy (Fig. 3). The peaks at 1632 cm^{-1} ($C{=}C_{ST}$) and 1196 cm^{-1} ($C{-}X_{ST}$)[16] attributable to the stilbene moiety are absent after ozonolysis, while a carbonyl stretch at 1700 cm^{-1} appears. This indicates that all surface and pore olefins present in the material have been modified.‡ Although CP MAS ^{13}C NMR was not sensitive enough to observe the aldehyde peak at 15% **1**, a material with 25% **1** does display an aldehyde peak at 197 ppm. Importantly, nitrogen adsorption analysis of the material following ozonolysis demonstrated that the ordered mesopore structure was unaffected by this treatment (see ESI†). The BET surface area increased slightly from 282 $m^2\ g^{-1}$ to 345 $m^2\ g^{-1}$ while the pore dimensions remain largely unaltered. This method demonstrates an ability to introduce a uniform reactivity to periodic mesoporous organosilica without pore reductions.

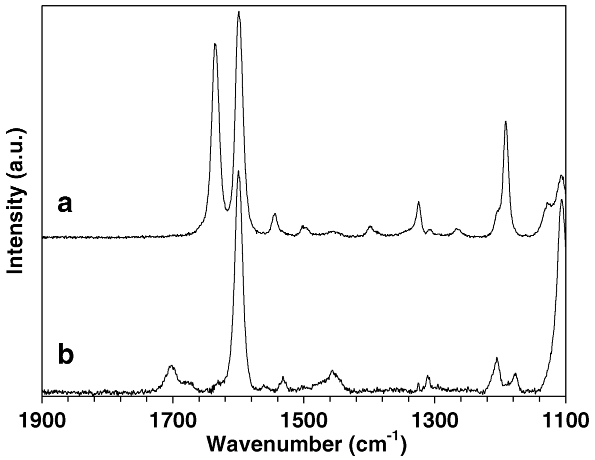

Fig. 3 Raman spectra of (a) **PMO-1/3$^{H^+}$** and (b) **PMO-1/3$^{H^+}$-O$_3$** showing complete consumption of C=C bond at 1632 cm^{-1}.

In summary, novel periodic mesoporous organosilica precursors have been synthesized containing both a functional and a structural component. The degree of homogeneity of the structural component was assessed from HAADF TEM images in tandem with EDX spectra. Reaction of the materials with ozone can be carried out without loss of mesoscale order, thanks to the presence of the structural units, while permitting the introduction of a well distributed, highly useful aldehyde functionality throughout the material. Further efforts to employ this group in subsequent transformations are underway.

The authors would like to thank Dr A. El Kadib for his contributions.

Notes and references

‡ The sampling volume of micro-Raman is sufficient to penetrate well into the porous mesostructure.

1 S. Inagaki, S. Guan, Y. Fukushima, T. Ohsuna and O. Terasaki, *J. Am. Chem. Soc.*, 1999, **121**, 9611; B. J. Melde, B. T. Holland, C. F. Blanford and A. Stein, *Chem. Mater.*, 1999, **11**, 3302; T. Asefa, M. J. MacLachlan, N. Coombs and G. A. Ozin, *Nature*, 1999, **402**, 867.
2 W. J. Hunks and G. A. Ozin, *J. Mater. Chem.*, 2005, **15**, 3716; F. Hoffmann, M. Cornelius, J. Morell and M. Fröba, *Angew. Chem., Int. Ed.*, 2005, **4**, 3216; M. P. Kapoor and S. Inagaki, *Bull. Chem. Soc. Jpn.*, 2006, **79**, 1463.
3 S. Inagaki, S. Guan, T. Ohsuna and O. Terasaki, *Nature*, 2002, **416**, 304; S. Fujita and S. Inagaki, *Chem. Mater.*, 2008, **20**, 891; K. Nakajima, I. Tomita, M. Hara, S. Hayashi, K. Domen and J. N. Kondo, *Adv. Mater.*, 2005, **17**, 1839; C. M. Li, J. Yang, X. Shi, J. Liu and Q. H. Yang, *Microporous Mesoporous Mater.*, 2007, **98**, 220; M. Cornelius, F. Hoffmann and M. Fröba, *Chem. Mater.*, 2005, **17**, 6674; T. Asefa, M. Kruk, M. J. MacLachlan, N. Combs, H. Grondey, M. Jaroniec and G. A. Ozin, *J. Am. Chem. Soc.*, 2001, **123**, 8520.
4 S. MacQuarrie, M. Thompson, A. Blanc, N. Mosey, R. P. Lemieux and C. M. Crudden, *J. Am. Chem. Soc.*, 2008, **130**, 14099.
5 X. Ding, X. Lv, B. Hui, Z. Chen, M. Xiao, B. Guo and W. Tang, *Tetrahedron Lett.*, 2006, **47**, 2921.
6 H.-K. Chang, S. Datta, A. Das, A. Odedra and R.-S. Liu, *Angew. Chem., Int. Ed.*, 2007, **46**, 4744.
7 M. Murata, M. Ishikura, M. Nagata, S. Watanabe and Y. Masuda, *Org. Lett.*, 2002, **4**, 1843.
8 H. Hopf, J. Hucker and L. Ernst, *Eur. J. Org. Chem.*, 2007, 1891; T. Bosanac and C. S. Wilcox, *Org. Lett.*, 2004, **6**, 2321.
9 W. J. Hunks and G. A. Ozin, *Chem. Commun.*, 2004, 2426.
10 M. P. Kapoor, Q. Yang and S. Inagaki, *J. Am. Chem. Soc.*, 2002, **124**, 15176.
11 Y. Goto and S. Inagaki, *Chem. Commun.*, 2002, 2410.
12 K. S. W. Sing, D. H. Everett, R. A. W. Haul, L. Moscou, R. A. Pierotti, J. Rouquerol and T. Siemieniewska, *Pure Appl. Chem.*, 1985, **57**, 603.
13 G. Cerveau, S. Chappellet, R. J. P. Corriu, B. Dabiens and J. L. Bideau, *Organometallics*, 2002, **21**, 1560.
14 Y. Yang and A. Sayari, *Chem. Mater.*, 2008, **20**, 2980.
15 D. Enders and O. Niemeier, *Synlett*, 2004, 2111.
16 X here represents *trans*-stilbene, less one aromatic ring. J. F. Arenas, I. L. Tocón, J. C. Otero and J. I. Marcos, *J. Phys. Chem.*, 1995, **99**, 11392.